# Interfacial Nanocomposite Characterization by Nanoparticle Debonding

J. Killgore and R. Overney*

*University of Washington, Seattle, WA, USA, roverney@u.washington.edu

## ABSTRACT

Heated tip AFM (HT-AFM) is an emerging scanning probe technique that can provide local transition behavior in polymer materials. We demonstrate here, that the tool also provides direct access to the interfacial interaction (debonding) strength in reverse selective nanocomposites of poly(trimethyl silyl propyne) (PTMSP) and silica. Local nano thermomechanical analysis identified a transition at 330°C, which subsequent imaging confirmed as degradation. By thermally inducing debonding of the silica particles, interfacial polymer mobility and debonding energy were simultaneously probed. Using a torsional stiffness calibrated thermal AFM probe, probe-particle impact force was continuously monitored to reveal a debonding force of 450 nN and an impact force transition 30°C below the degradation temperature in the neat polymer, confirming the presence of enhanced polymer mobility at the PTMSP-silica interface.

***Keywords***: HT-AFM, interface, debonding, nanocomposite, poly(trimethylsilyl propyne)

## 1 INTRODUCTION

Poly(trimethyl silyl propyne) (PTMSP) blended with nano-scale silica particles is a composite system which has garnered significant attention for it's unique properties.[1, 2] Specifically, when used as a gas membrane, PTMSP exhibits reverse selectivity, thereby showing higher permeability to large soluble gases than for small permanent gases. Typically it is expected that the introduction of an impermeable filler material will result in a corresponding volumetric decrease in permeability,[3] which is further amplified by an increase in diffusing path length.[4] However, in the case of PTMSP and silica, enhanced permeability with increased filler concentration is observed. Furthermore, large molecule to small molecule selectivity is also enhanced.[5, 6] The significant permeability enhancement, even with a large concentration of an impermeable phase, suggests that physical or chemical alteration of the polymer has occurred at the composite interface.

Molecular dynamics simulations have demonstrated that Si-SiO2 induced electrostatic repulsion between the polymer and particle results in enhanced mobility of the interfacial PTMSP.[7] Enhanced mobility creates lower density regions around the interface, allowing for faster gas molecule diffusion. This calculation has been supported experimentally by bulk positron annihilation lifetime spectroscopy (PALS), which showed an increase in free volume domain size from 1.4 nm at 0% SiO2 to 1.44 nm at 25% SiO2 loading.[8] Assuming these subdomains remain discrete, permeation obeys solution-diffusion behavior similar to the neat polymer; however, if increased particle loading results in a series of interconnected subdomains, Knudsen type flow becomes significant, and reverse selective behavior begins to break down.

In an effort to better understand the interfacial properties of PTMSP-silica composites, heated tip atomic force microscopy (HT-AFM) is used here to study the adhesive strength between PTMSP and silica nanoparticles. Although initially developed for local nano thermomechanical analysis (nTMA),[9-12] it has recently been shown that resistively heated nanoscopically sharp cantilever probes provide the opportunity to study adhesive interactions between the polymer matrix and a single silica particle.[13] Here, discrete measurements and observations on individual particles allow for comparison of particle size effects and measurement of debonding energy. Furthermore, mobility of the interface is explored by comparison of debonding temperatures with local neat polymer transition temperature measurements.

## 2 EXPERIMENTAL

### 2.1 Materials

PTMSP was obtained from Gelest, Inc. and dissolved into a 2 % solution in toluene. Silica particles of 190 nm diameter were prepared by mixing 200 ml anhydrous ethanol, 6 ml tetraethyl orthosilicate and 12 ml of 30 wt% ammonia in water in a glass beaker for 12 hours. The solution was then dried to produce a silica powder. Trace amounts of the dry silica powder were ultrasonically mixed into the polymer solution, which was then added drop wise to a clean glass slide and dried for 7 days in a fume hood.

### 2.2 Characterization

HT-AFM measurements were performed using a Topometrix Explorer SPM with heated probes provided by Anasys Inc., with tip radii of ~30 nm and normal spring constants of ~1 N/m. The input voltage was generated from a 10 V National Instruments data acquisition card, and custom electronics allowed for real time monitoring of tip voltage and current.



NSTI-Nanotech 2008, www.nsti.org, ISBN 978-1-4200-8503-7 Vol. 1

Calibration of the HT-AFM probe was completed as follows. After performing a topography scan of the sample, the probe was positioned on a suitable surface location and the SPM feedback controller disabled. The power to the heater was ramped at a rate of 1.2 V/min until a transition in the cantilever normal deflection signal was observed. Below the melt temperature, the signal increases steadily as a result of the coupled thermal expansion of the tip and the sample. At the transition temperature, the tip penetrates the sample, as indicated by a rapid decrease in the Z-signal (or change in slope as in PI). The melt/glass transition temperature values for polycaprolactone (PC) ($T_m$ = 60 °C), polyethylene (PE) ($T_m$ = 130 °C), polyethylene terephthalate (PET) ($T_m$ = 238 °C) and polyimide (PI) ($T_g$ = 333 °C) were correlated to HT-AFM input voltage with a sigmoidal fit. By comparing to SM-FM, a well-established surface $T_g$ probing technique that allows the use of SPM levers,[14, 15] we found the HT-AFM calibration in good correspondence on polystyrene.

Heated scans were performed with a constant heater temperature setting. Coarse 200 line 10 μm scans were performed at a scan speed of 20 μm/s with a normal force of ~23nN. Temperatures were ramped in 10 °C increments until significant surface deformation was observed. Subsequently, in a new area, 200 line, 1.5 μm scans were used to provide a detailed analysis of specific particles. For each scan, the normal Z-piezo voltage, the normal lever deflection signal, and the forward and reverse lateral force signals were recorded.

## 2.3 Debonding Analysis

Figure 1 shows a representative forward direction line trace for the lateral deflection signal. The deflection, as the cantilever impacts an embedded particle, is described by magnitude, $\Delta F_{max}$ and duration, α. $\Delta F_{max}$ and α are recorded at each temperature from the forward and reverse lateral force signals and compared to the baseline polymer-particle signal, β. Lateral deflection was converted to units of force using the blind calibration technique of Buenviaje et al. on a surface of known friction coefficient (Si <1,1,1>).[16]

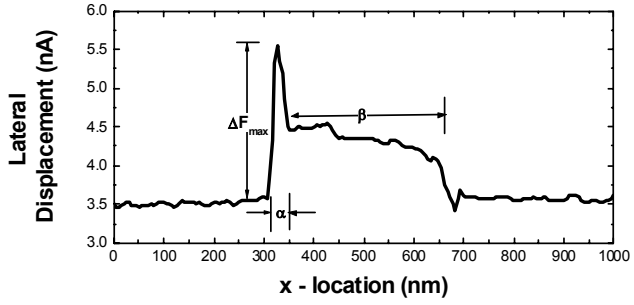


Figure 1. Lateral force line trace of polymer embedded silica nanoparticle.

# 3 RESULTS AND DISCUSSION

## 3.1 Transition Analysis

In contrast to most other glassy polymers that exhibit glass transitions at temperatures significantly below their degradation temperature, PTMSP exhibits a complex thermal relaxation behavior wherein degradation precedes the glass transition.[17] Thus, a true glass to rubber transition has not been recorded in the literature, but it is generally accepted to be in excess of 250°C.[18] Figure 2 shows a HT-AFM thermal transition plot on a PTMSP film, revealing a transition temperature, T* of 330 °C, which exceeds the degradation onset.[17]

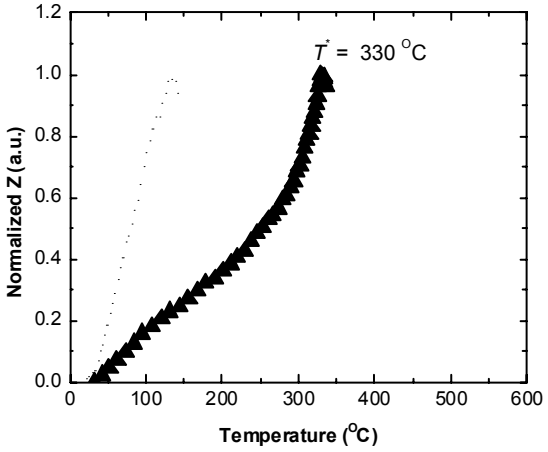


Figure 2: HT-AFM thermal analysis plot on PTMSP. Transition temperature is indicated by the apex of the tip displacement curve.

Subsequent to indentation, by scanning the probed area, HT-AFM also provides information about thermally-induced mechanical indentation properties, and thus provides an opportunity to contrast degradation with a glass transition process. The hole pattern in PTMSP exhibited no plastic rim formation, suggesting that the very rigid conjugated backbone of PTMSP is still highly resistant to deformation at $T^*$ = 330 °C. This suggests that the critical transition in PTMSP is due to decomposition, which consequently preceded the glass transition.

## 3.2 Particle Debonding – Coarse Scanning

Figure 3(a) and (b) provide 10 μm HT-AFM topography scans at room temperature on PTMSP, recorded before (a) and after (b) a series of scans at probe temperatures up to 336 °C that caused particles to debond from the surface at critical conditions (temperature, pressure and scan rate). Comparing the surface particle density in the two images,

there are considerably fewer particles in the post heated scanning image. The debonding occurred at a range of temperatures from ~5 °C below to 5 °C above T*. It should be noted that upon impact of the HT-AFM probe with the silica particle, the probe temperature is expected to be lower than the actual tip temperature as heat is removed by the particle. The magnitude is however to be considered small and within the provided debonding range around T*.

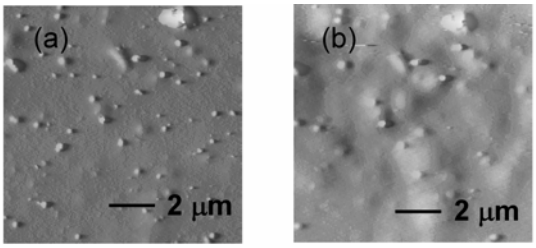


Figure 3. (a) and (b) Room temperature 10 μm HT-AFM topography scans on PTMSP before and after heated scanning respectively.

## 3.3 Scan Size Effect.

At the same scan frequency, compared to the 10 μm scans discussed above, a 1.5 μm scan results in a larger number of particle impacts per scan (same scan resolution over a smaller area) and an increased equilibrium contact temperature (slower scan speed). Figure 4 shows a silica aggregate in PTMSP before and after heated scanning. A particle height of ~100 nm was measured prior to debonding, while a 40 nm cavity with an additional 20 nm rim was observed after debonding. The particle satisfies the earlier specified conditions of shallow embedding and high topography, allowing debonding to occur at a temperature of 326 °C, consistent with the lower bound debonding temperatures from the 10 μm scans.

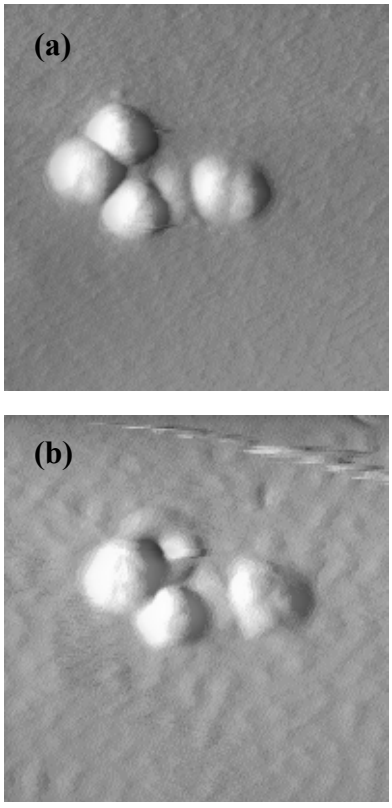


Figure 4. 1.5 μm debonding scans on PTMSP before, (a), and after, (b), heated scanning at 326 °C.

## 3.4 Debonding Forces.

Investigation of lateral impact forces, i.e., the lateral peak forces $\Delta F_{max}$ (see Fig. 1), on silica in PMMA and PTMSP reveal dramatically different thermal responses in the vicinity of the transition temperature. As shown in Figure 5, the impacting force $\Delta F_{max}$ for PTMSP decreases slowly from 200 nN at room temperature to 50 nN at ~300 °C, before it sharply increases to ~450 nN prior to debonding at $T_{DB}$, 326 °C. Softening creates a feedback delay as the probe impacts the particle, and ultimately induces greater torsional deflection of the lever. The onset of the force increase is attributed to the local transition behavior of PTMSP at the particle interface. The onset, T', occurs ~30 °C below T*. The critical temperature T', above which adhesive failure is noticeable, provides insight into the mobility of the polymer phase in close vicinity to the particle. As adhesive failure under such slow sliding conditions and fast normal force feedback control can be expected to be dominated by transition properties, and as $T' < T^* < T_g$, we can conclude that the polymer matrix in the interfacial region possesses increased mobility. This confirms current models, based on global free volume measurements, that showed an increase in free volume on average over the bulk composite.[8] Thus, the experimentally observed increase in polymer matrix


NSTI-Nanotech 2008, www.nsti.org, ISBN 978-1-4200-8503-7 Vol. 1

mobility in the interfacial region allows for the formation of larger free volume cavities which contribute to increased local sorption and diffusion. It can also be concluded, based on the direction of the interfacial transition temperature change, that a repulsive interface is present.[19]

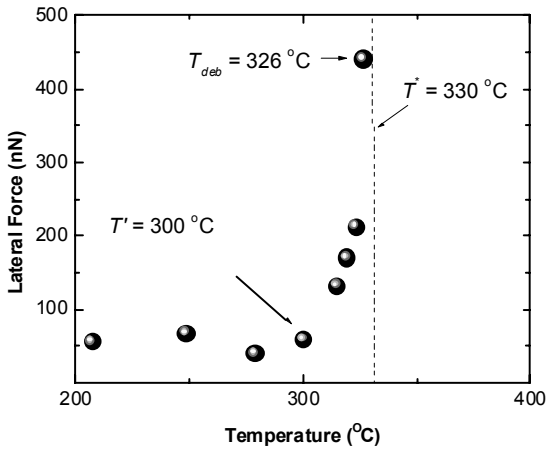


Figure 5. Debonding force $\Delta F_{max}$ to remove silica particles embedded in PTMSP as function of the probe temperature.

## 4 CONCLUSION

In addition to local transition property analysis, HT-AFM provides direct access to manipulation of isolated particles in nanocomposite thin films. Local thermal analysis with subsequent imaging yielded a transition of 330 °C that was found to be caused by thermal degradation. The study and manipulation of embedded nanoparticles in PTMSP revealed an impact force transition temperature ~30°C below the measured degradation transition, suggesting the presence of more mobile polymer chains at the particle interface. This is an interesting finding as the properties of the interfacial region are responsible for the enhanced mass transfer properties of the PTMSP-silica composite over virgin PTMSP. The debonding strength of single particles with the polymer matrix, which offers a simple measure of the interface, was determined to be 450 nN.

## REFERENCES


1. Pinnau, I. and L.G. Toy, Journal of Membrane Science, 1996. **116**(2): p. 199-209.
2. Nagai, K., et al., Progress in Polymer Science, 2001. **26**(5): p. 721-798.
3. Barrer, R.M., *Diffusion and Permeation in Heterogeneous Media*, in *Diffusion in Polymers*, A. press, Editor. 1968: London.
4. Bharadwaj, R.K., Macromolecules, 2001. **34**(26): p. 9189-9192.
5. Merkel, T.C., et al., Macromolecules, 2003. **36**(18): p. 6844-6855.
6. De Sitter, K., et al., Journal of Membrane Science, 2006. **278**(1+2): p. 83-91.
7. Zhou, J.-H., et al., Polymer, 2006. **47**(14): p. 5206-5212.
8. Hill, A.J., et al., Journal of Molecular Structure, 2005. **739**(1-3): p. 173-178.
9. Reading, M., et al., American Laboratory (Shelton, Connecticut), 1998. **30**(1): p. 13-17.
10. Reading, M., et al., American Laboratory (Shelton, Connecticut), 1999. **31**(1): p. 13-16.
11. Grandy, D. and K. Kjoller, Microscopy Today, 2006. **14**(4): p. 58,60.
12. Pollock, H.M. and A. Hammiche, Journal of Physics D: Applied Physics, 2001. **34**(9): p. R23-R53.
13. Gray, T., et al., Nanotechnology, 2007. **18**.
14. Ge, S., et al., Physical Review Letters, 2000. **85**(11): p. 2340-2343.
15. Sills, S., et al., J. Chem. Phys., 2004. **120**(11): p. 5334-5338.
16. Buenviaje, C.K., et al., Materials Research Society Symposium Proceedings, 1998. **522**(Fundamentals of Nanoindentation and Nanotribology): p. 187-192.
17. G. Consolati, I.G., M. Pegoraro, L. Zanderighi,, Journal of Polymer Science Part B: Polymer Physics, 1996. **34**(2): p. 357-367.
18. Hill, A.J., et al., Journal of Membrane Science, 2004. **243**(1-2): p. 37-44.
19. Fryer, D.S., et al., Macromolecules, 2001. **34**(16): p. 5627-5634.